

Exact analytical solutions for steady three-dimensional inviscid vortical flows

S. BHATTACHARYA

Department of Mechanical Engineering, Texas Tech University, Lubbock, TX 79409, USA

(Received 3 August 2006 and in revised form 13 June 2007)

Vortical flows with an axial (z -axis) swirl and a toroidal circulation (in the (ρ, z) -plane) can be observed in a wide range of fluid mechanical phenomena such as flow around rotary machines or natural vortices like tornadoes and hurricanes. In this paper, we obtain exact analytical solutions for a general class of steady systems with such three-dimensional circulating structures. Assuming incompressible ideal fluid, a general single-variable equation, known as the Squire–Long equation, can be constructed which can uniquely describe the velocity fields with steady axial and toroidal circulations. In this paper, we consider the case where this type of flow can be analysed by solving a linear homogeneous partial differential equation. The derived equation resembles the governing equation of the hydrogen problem. As a result, we obtain a quantization relation which is similar to the expression for the quantized energy states in a hydrogen atom.

For circulating flows, this formalism provides a complete set of orthogonal basis functions which are regular and localized. Hence, each of the basis solutions can be used as a simplified model for a realistic phenomenon. Moreover, an arbitrary circulating field can be expanded in terms of these orthogonal functions. Such an expansion can be potentially useful in the study of more general vortices. As illustrations, we present a few examples where we solve the linear homogeneous equation to analyse fluid mechanical systems which can be models for circulating flow in confined geometry. First, we consider three-dimensional vortices confined between two parallel planar walls. Our examples include flows between two infinite planar walls, inside and outside a vertical cylinder bounded at the ends by horizontal plates, and in an axially confined annular region. Then we describe the special way in which the basis functions should be superposed so that a complicated steady velocity-field with three-dimensional vortical structures can be constructed. Two such cases are discussed to indicate that the derived solutions can be used for complicated fluid mechanical modelling.

1. Introduction

Vortical flow is a common feature in many fluid mechanical systems where the circulating velocity field plays an important role. Such flow exists in nature in the forms of hurricanes and tornadoes. Other examples are the velocity fields generated around rotary machines such as propellers, fans or windmills. Hence, for both science and technology, it is necessary to analyse the dynamics of such a vortical circulation, which generally involves a complicated three-dimensional field.

The length scales and the time scales associated with the aforementioned systems are very different in each case. However, there are a few underlying similarities and common characteristics in these vortical flows. First of all, these phenomena can

be considered quasi-steady in the time scale of the predominant vortices (Bragg & Hawthorne 1950; Batchelor 1964; Sozou, Wilkinson & Shtern 1994). These are all high-Reynolds-number flows so that the viscous effect can be neglected for the velocity field away from a solid boundary (Moffat 1981; Buntine & Saffman 1995). Moreover, all of these involve two major circulations: one is about an axis of swirl (which may be denoted as the z -axis) and the second is a toroidal circulation in the (ρ, z) -plane where ρ is the distance from the axis of swirl. The velocity fields in hurricanes (Emanuel 1991) and tornadoes (Ward 1972; Burggraf & Foster 1977; Keller 1994) or the flows produced by rotating machines (Escudier 1984, 1987; Lopez 1998) exhibit such generic vortical structures.

Besides their presence in large-scale-flow phenomena, these structures also exist in the form of localized eddies in turbulent phenomena. Because of the divergenceless velocity and vorticity, the streamlines and vortex-lines of any localized vortex must be closed loops. Hence, the eddies in turbulence often form local velocity fields which resemble the flow patterns with both axial and toroidal circulations (Gollub & Swinney 1975; Malik & Chang 1994). Thus, the understanding of a wide range of fluid mechanical systems depends on a thorough knowledge of such fundamental structures.

In this paper, we derive expressions for steady inviscid vortical flows by solving a linear homogeneous partial differential equation. These analytical results have qualitative agreement with the fluid mechanical measurements in high-Reynolds-number systems where vorticity is generated in a confined domain. For example, experiments involving propellers (Lepicovsky & Bell 1984; Fukada, Nigim & Koyama 1996) and vortex simulators (Church *et al.* 1979; Mitsua & Monji 1984) show agreement with the theoretically calculated streamlines. Hence, the solutions presented can be useful in the modelling of such vortical systems.

There are several known exact results where either the full Navier–Stokes equation with the viscous term or the inviscid Euler equation is solved to analyse swirling flows. Examples include the vortices described by Hill (1894) and by Lamb (1945). More recently, exact solutions have been proposed for different types of circulations (Wang 1991; Saffman 1992; Bazzant & Moffat 2005; Le Dizès & Lacaze 2005). There are also related theoretical and numerical works involving axisymmetric swirling jets (Long 1961; Fernandez-Feria, de la Mora & Barrero 1995), vortex breakdown (Goldshik & Shtern 1990; Shtern & Hussain 1999) and vortical instabilities (Gelfgat, Bar Yoseph & Solan 1996; Delbende, Chomaz & Huerre 1998). These past studies, however, substantially differ from our analysis.

In spite of these exact solutions, there are few analytical results where a swirling flow with complicated three-dimensional structures was considered. The small number of available solutions for such flows invariably involve a singularity in the flow domain. This somewhat restricts the prospect of these results being used in modelling of circulations in a confined domain. In contrast, the expressions derived in this paper, though corresponding to a steady inviscid flow, describe three-dimensional velocity fields which are regular and localized. Hence, they can be good models for the vortices with axial and toroidal swirl, and provide bench-marks for validation of numerical schemes under limiting conditions. Moreover, the obtained solutions form a complete basis set in which complicated velocity fields can be expanded. Such expansions can be potentially useful to simulate large-scale vortices with temporal variation and viscous effects.

The paper is organized in the following way. In §2, we present the general solutions for the circulating flow with axial and toroidal swirls. In §3, we identify the

non-dimensional groups which define the vortical system and discuss a few specific examples in terms of these parameters. If the solutions are superposed in a specific manner, they can describe a steady velocity field with complicated patterns. Details of this superposition technique and examples of complex flow structures are presented in §4. Finally, conclusions are drawn in §5.

2. A general set of solutions for steady inviscid vortical flow

The mass and the momentum conservation equation for velocity fields with both axial swirls and toroidal circulations can be simplified by considering incompressible fluid and negligible viscous dissipation. The equations are expressed in cylindrical coordinates (ρ, ϕ, z) . The components of velocity \mathbf{v} in the directions of the respective coordinates are v_ρ, v_ϕ, v_z , all of which are, in general, non-zero. We assume that:

$$\frac{\partial}{\partial \phi} = 0 \implies \frac{\partial v_\rho}{\partial \phi} = \frac{\partial v_\phi}{\partial \phi} = \frac{\partial v_z}{\partial \phi} = \frac{\partial p}{\partial \phi} = \frac{\partial V}{\partial \phi} = 0, \quad (2.1)$$

where p is the pressure field and V is an external potential.

2.1. The simplified governing equation for the system

Under these conditions, the fluid mechanical equations can be simplified into a single variable equation which is known as the Squire–Long equation (Fraenkel 1956; Squire 1956; Long 1961). In order to do so, the solenoidal velocity field is expressed in terms of two scalar streamfunctions ψ_1 and ψ_2 :

$$\mathbf{v} = \nabla\psi_1 \times \nabla\rho + \nabla\psi_2 \times \nabla\phi = -\frac{1}{\rho} \frac{\partial\psi_2}{\partial z} \hat{\mathbf{e}}_\rho + \frac{\partial\psi_1}{\partial z} \hat{\mathbf{e}}_\phi + \frac{1}{\rho} \frac{\partial\psi_2}{\partial\rho} \hat{\mathbf{e}}_z. \quad (2.2)$$

Then, replacing \mathbf{v} in the momentum equation in terms of ψ_1 and ψ_2 , it can be shown that the conserved quantities such as total specific energy e and axial specific angular momentum f are explicit functions of ψ_2 :

$$\mathbf{v} \cdot \mathbf{v}/2 + p/d + V = e(\psi_2), \quad \rho^2 \mathbf{v} \cdot \nabla\phi = f(\psi_2), \quad (2.3)$$

where d is the fluid density. The explicit functions $e(\psi_2)$ and $f(\psi_2)$ can take any form and each case corresponds to a different flow.

Hence, we can decouple e and ψ_1 from ψ_2 though all three variables are coupled in the original momentum equation. As a result, it is possible to convert the multivariable flow problem into a single scalar equation. This scalar equation is known as the Squire–Long equation (Squire 1956; Long 1961):

$$\nabla \cdot \left(\frac{1}{\rho^2} \nabla\psi_2 \right) + \frac{f(\psi_2)f'(\psi_2)}{\rho^2} - e'(\psi_2) = 0, \quad (2.4)$$

which along with (2.3) describes the dynamics of the circulating flow. The two explicit functions e and f can be determined either by measurements or by modelling; but whatever their functional forms may be, the obtained solution will always satisfy the mass and the momentum conservation equations.

2.2. The linear model

The presented formulation can provide a solution for numerous types of vortical fields. The solution depends on the functional form of $e(\psi_2)$ and $f(\psi_2)$ which can vary from model to model for different flows. Among all possible cases, in this paper, we analyse a specific case where the problem can be associated with a linear homogeneous equation.

For our systems, we consider the relations:

$$e = c + \frac{1}{2}\beta^4\psi_2^2, \quad (2.5)$$

$$f = \lambda\psi_2. \quad (2.6)$$

Here, β and λ are two constants whose inverses are two important length scales related to the distribution of the energy and the angular momentum of the vortical flow. The form of the two explicit functions in (2.5) and (2.6) differ from those adopted in previous studies (Fraenkel 1956; Squire 1956; Long 1961). As a result of our model selection, (2.4) can be converted into a linear homogeneous equation for ψ_2

$$\frac{\hat{L}(\psi_2)}{\rho^2} = \nabla \cdot \left(\frac{1}{\rho^2} \nabla \psi_2 \right) = \beta^4 \psi_2 - \frac{\lambda^2}{\rho^2} \psi_2, \quad (2.7)$$

where the Stokes operator $\hat{L} = \rho^2 \nabla \cdot (1/\rho^2 \nabla)$. In this paper, we focus on solving (2.7).

2.3. Separable solutions

Separable solutions for (2.7) are conceived to be of the following form:

$$\psi_2 = g(z)H(\beta^2\rho^2) = g(z)H(\eta), \quad (2.8)$$

where g and H are two functions, and $\eta = \beta^2\rho^2$. Then, considering that ψ_2 is finite for all z , we find

$$g''(z) = -k^2g(z) \implies g(z) = e^{\pm ikz}. \quad (2.9)$$

Accordingly, H satisfies

$$4H'' + 4\nu \frac{H}{\eta} - H = 0, \quad (2.10)$$

where

$$\nu = \frac{\lambda^2 - k^2}{4\beta^2} \quad (2.11)$$

is a non-dimensional parameter.

For the flow to be physical, H has to be finite for all η and should decay to zero when $\eta \rightarrow \infty$. To this end, we consider the decaying asymptotic behaviour of (2.10):

$$4H'' - H = 0|_{\eta \rightarrow \infty} \implies H = e^{-\eta/2}|_{\eta \rightarrow \infty} \quad (2.12)$$

and define a new function which describes the departure from the asymptotic behaviour

$$h = H e^{\eta/2} \quad \text{or} \quad H = h e^{-\eta/2}. \quad (2.13)$$

When (2.10) and (2.13) are combined, the equation for $h(\eta)$ turns out to be related to the Laguerre equations

$$h'' - h' + \nu \frac{h}{\eta} = 0, \quad (2.14)$$

so that the solution for h is an integral of the Laguerre polynomial of order $\nu - 1$. To distinguish between different solutions for different values of ν , we denote h in the above equation as h_ν .

2.4. Quantization relation

In general, h_ν can be expressed as a polynomial series

$$h_\nu = \sum_{i=1}^{\nu} a_i^{(\nu)} \eta^i, \quad (2.15)$$

where the coefficients satisfy the following recurrence relation:

$$a_{i+1}^{(v)} = -\frac{v-i}{i(i+1)}a_i^{(v)}. \quad (2.16)$$

In order to obtain a physical solution, this polynomial must be truncated at some finite term. In this respect, the mathematical formulation of the linear model for vortical flows has a remarkable similarity with the formulation of the hydrogen problem in quantum mechanics (Griffiths 1994). In both cases, the non-dimensional parameter ν involved in the Laguerre equation has to be a positive integer:

$$\nu = 1, 2, 3 \dots. \quad (2.17)$$

Therefore, the values of λ , β and k are constrained by a quantization relation:

$$\lambda^2 - k^2 = 4n\beta^2, \quad (2.18)$$

where, n is any positive integer. Therefore, if a circulating flow corresponds to the proposed linear model, then the chosen proportionality constants in (2.5) and (2.6) have to comply with (2.18) and cannot assume arbitrary values independently. This constraint is similar to the relation for the quantized energy levels of a hydrogen atom.

For different values of n , we obtain different polynomial functions represented as h_n . The corresponding flow is referred to as the flow of the n th radial mode. A few of the polynomial functions for the first few values of n are given below:

$$h_1 = \eta, \quad h_2 = \eta - \frac{\eta^2}{2}, \quad h_3 = 2\eta - 2\eta^2 + \frac{\eta^3}{3}, \quad h_4 = 6\eta - 9\eta^2 + 3\eta^3 - \frac{\eta^4}{4}. \quad (2.19)$$

These expressions along with (2.2), (2.5), (2.6), (2.8), (2.9) and (2.13) completely describe the velocity and the pressure field for the three-dimensional circulations.

3. Vortical flows between two parallel walls

We use the mathematical solutions derived in the previous section to describe circulating velocity fields confined between two parallel impermeable walls. The walls are represented by surfaces at $z=0$ and $z=b$, where b is the height of the channel.

In such geometry, the impermeability condition at the walls can be satisfied only if $\psi_2=0$ at these surfaces. Hence, ψ_2 for the vortical flow-field of the n th-order radial mode has the following form:

$$\psi_2 = A \sin(m\pi z/b)h_n(\eta)e^{-\eta/2}, \quad (3.1)$$

where A is an amplitude and m can take any integer value. However, the solution corresponding to $m=1$ is the most important and fundamental one since for all other values of m , the solutions can be conceived as a repetition of the fundamental solution with $m=1$ in a channel of height b/m . Hence, in our analysis, we only consider $m=1$ and

$$\psi_2 = A \sin(\pi z/b)h_n(\eta)e^{-\eta/2}. \quad (3.2)$$

3.1. Energy and angular momentum of confined vortices

In (3.2), the amplitude A is an unknown parameter. According to our formulation, the governing equation and the boundary conditions for ψ_2 are homogeneous, and as a result cannot provide the value of the amplitude. Moreover, for the description of any physical flow, the proportionality constants β and λ defined in (2.5) and (2.6)

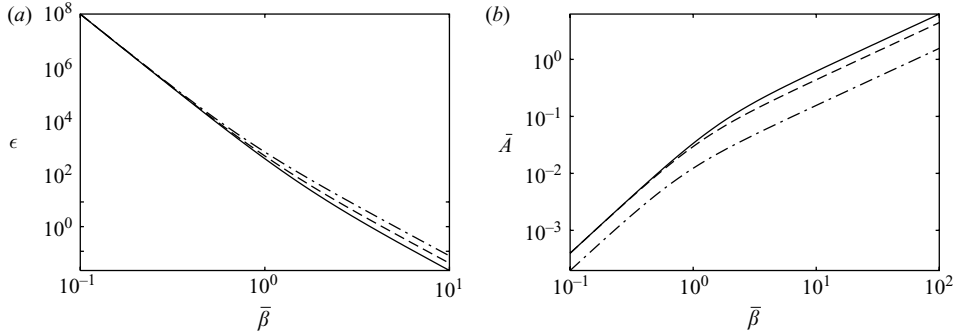


FIGURE 1. Plots of (a) ϵ and (b) \bar{A} as functions of $\bar{\beta}$ for $n=1$ (solid line), $n=2$ (dashed line) and $n=3$ (dash-dotted line).

have to be evaluated. Therefore, we require three additional constraints to determine A , β and λ . One of the three constraints is the quantization relation (2.18) which gives a relation between β and λ . The remaining two required relations can be obtained from simple physical arguments.

The total energy E and the total angular momentum L_z in the z -direction of a confined non-dissipative vortex are two conserved quantities. These two known conserved quantities give the two necessary inhomogeneous conditions for evaluation of not only the amplitude, but also β and λ for a vortex of the n th-order radial mode. To this end, we define a few non-dimensional quantities to describe properly the relations among the relevant quantities. For example, β and λ are non-dimensionalized with the help of channel width b

$$\bar{\beta} = b\beta, \quad \bar{\lambda} = b\lambda. \quad (3.3)$$

Similarly, two other non-dimensional groups involving A , L_z and E are as below

$$\bar{A} = \frac{db^2A}{L_z}, \quad (3.4)$$

$$\epsilon = \frac{L_z^2}{db^5E}. \quad (3.5)$$

The quantization relation can then be used to express $\bar{\lambda}$ in terms of $\bar{\beta}$:

$$\bar{\lambda} = \pm \sqrt{4n\bar{\beta}^2 + \pi^2}. \quad (3.6)$$

The other two required relations among $\bar{\beta}$, \bar{A} and ϵ can be obtained in the form $\bar{A} = \bar{A}(\bar{\beta}, n)$ and $\epsilon = \epsilon(\bar{\beta}, n)$ by evaluating the integrals of ψ_2^2 and ψ_2 in expressions representing the energy and the angular momentum of the system given by (2.5) and (2.6).

We calculate these integrals and present ϵ and \bar{A} as functions of $\bar{\beta}$ for different values of n in figure 1. When $\beta \rightarrow 0$ and $\beta \rightarrow \infty$, the log-log plots reveal the limiting values of ϵ and \bar{A} ($\epsilon \sim \bar{\beta}^{-6}$, $\bar{A} \sim \bar{\beta}^2$ for $\beta \rightarrow 0$ and $\epsilon \sim \bar{\beta}^{-4}$, $\bar{A} \sim \bar{\beta}$ for $\beta \rightarrow \infty$). These plots can be used to assign proper values to the unknown parameters for the vortical system. For given E and L_z , ϵ is known. Hence, from the ϵ - $\bar{\beta}$ plot, we can determine $\bar{\beta}$ for a field with radial mode n . Then, the value of $\bar{\beta}$ can be used in the \bar{A} - $\bar{\beta}$ plot to find the corresponding dimensionless amplitude for the vortex.

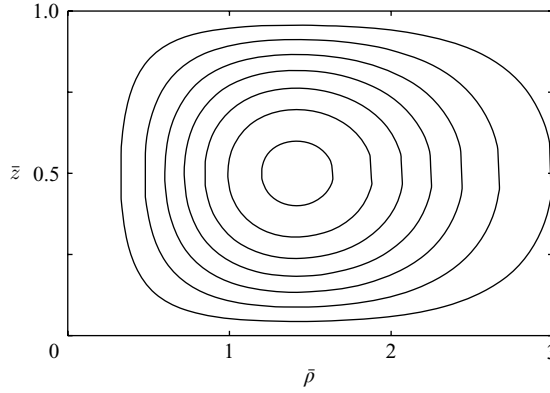


FIGURE 2. Projections of streamlines on the (ρ, z) -plane for a vortex with axial and toroidal swirls trapped between two infinite parallel plates. This vortex corresponds to the radial mode $n = 1$.

The dimensional analysis quantifies the proper scales for distance, time and velocity associated with the vortex. As a result, we can predict the diffusion time scale t_d for which this inviscid solution remains valid for a large but finite Reynolds number Re . If Re is large but finite, the total head decreases with time owing to the viscous dissipation and the solution varies slowly with time. The time scale of such slow temporal variation is equal to t_d . This time scale depends on the value of $\bar{\beta}$. If $\bar{\beta} \ll 1$, the time scale for vorticity diffusion is b^2/ν . On the other hand, if $\bar{\beta} \gg 1$, then $t_d = 1/(\nu\bar{\beta}^2)$.

3.2. Circulating flow between two infinite parallel plates

When the radial mode n is unity, the solution for the streamfunction described by (3.2) corresponds to the vortex with axial and toroidal swirls in a space between two infinite parallel plates. In order to analyse the detailed solution for such a velocity field, we define the following dimensionless quantities:

$$\bar{z} = z/b, \quad \bar{\rho} = \beta\rho, \quad (3.7)$$

$$\bar{v}_\rho = \frac{v_\rho b}{\beta A}, \quad \bar{v}_\phi = \frac{v_\phi}{\lambda\beta A}, \quad \bar{v}_z = \frac{v_z}{\beta^2 A}, \quad (3.8)$$

$$\bar{p} = \frac{2}{d\beta^4 A^2} p. \quad (3.9)$$

We present our results in terms of these dimensionless variables.

The projections of streamlines in the (ρ, z) -plane describe the structure of the toroidal circulation. These projection lines are shown in figure 2 to elucidate the direction of the velocity field in the ρ and z directions. The projected streamlines are closed loops to ensure mass conservation in a bounded domain. The figure indicates that at $\bar{\rho} = 1.414$ the velocity is entirely in the angular direction and that point acts as a stagnation point for the circulation in the (ρ, z) -plane.

Figure 3 specifies the components of the velocity vector in the ϕ and z directions. The variations in v_ϕ and v_z are proportional to $\sin(\pi\bar{z})$ for fixed $\bar{\rho}$. The amplitudes of these two sinusoidal quantities are presented in figure 3 as functions of $\bar{\rho}$. The plots show that at the axis of symmetry, the velocity in the angular direction goes to zero whereas v_z is maximum at the same position. Then v_ϕ reaches a maximum value as $\bar{\rho}$ increases and eventually decays to zero for $\bar{\rho} \rightarrow \infty$. On the contrary, v_z decreases

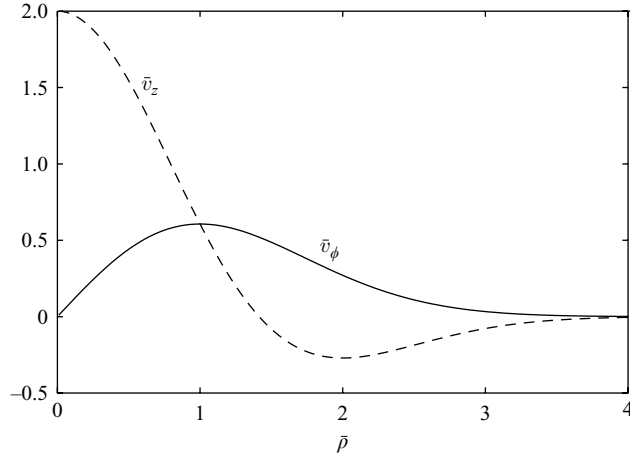


FIGURE 3. Non-dimensional components of the velocity field with radial mode $n=1$ are presented as functions of non-dimensional radial distance. The curves correspond to the flow at the midsection of the channel ($\bar{z}=1/2$).

gradually to zero and then to negative values to ensure mass conservation for the flow trapped by two impermeable walls.

Figure 4 presents the dimensionless pressure as a function of $\bar{\rho}$ and \bar{z} for different values of $\bar{\beta}$. The velocity is less near the wall and as a result the pressure is more for $z=0$. Similarly, higher values of $\bar{\beta}$ cause the velocity head to be weaker than the pressure head which is evident from the figures. These observations are consistent with Bernoulli's principle where an increase in velocity causes a decrease in pressure.

3.3. Vortex confined by cylindrical surfaces and planar walls

The higher-order radial modes (such as $n=2, 3, \dots$) in (3.2) correspond to flow fields which are bounded by horizontal planar surfaces and vertical cylindrical boundaries. Depending on the value of n and the region of interest, this axially bounded domain may be either inside or outside an impermeable cylinder or inside an annular space.

The radial functions $h_n(\bar{\rho})$ in (2.19) vanish for $n-1$ distinct non-zero values of $\bar{\rho}$. Hence, for such values of $\bar{\rho}$, ψ_2 is zero and the corresponding cylindrical surface represents an impermeable vertical boundary. Thus, for the n th-order radial mode, the flow field is divided into n subdomains in which disconnected circulations are contained.

We present projections of the streamlines in the (ρ, z) -plane for $n=2$ and $n=3$ in figure 5 to illustrate the toroidal circulations. The plots indicate the segmented flow domains. For $n=2$, a single impermeable cylinder divides the flow in two subdomains at $\bar{\rho}=1.26$. These subdomains are denoted as inside and outside of the cylinder in the figure. For $n=3$, there are two such cylindrical surfaces at $\bar{\rho}=1.14$ and $\bar{\rho}=2.17$. Hence, there are three subdomains: the first one is inside the first cylinder, whereas the second is the annular region in between the two cylinders and the third is outside the second cylinder. In all cases, for $\bar{\rho} \rightarrow \infty$ the velocity fields exponentially decay to zero.

3.4. Stability analysis

The physical behaviour of the vortical systems corresponding to the derived solutions depends on the stability of the described fields. Hence, we present a stability analysis of these flows by using Arnol'd's well-known stability theorem (Arnol'd 1966a, b).

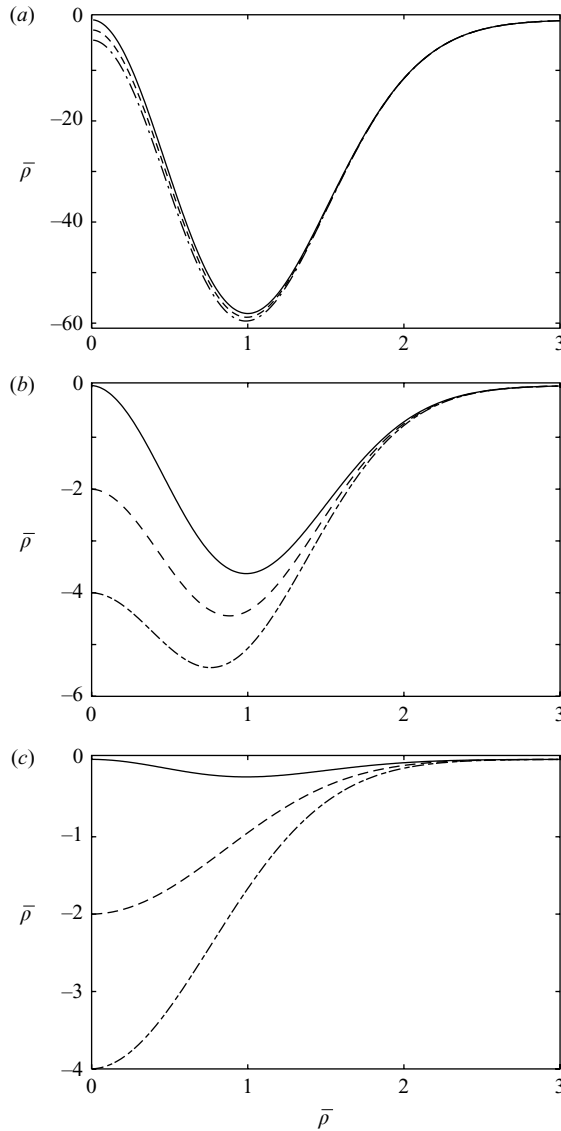


FIGURE 4. Non-dimensional pressure for the vortical flows with $n = 1$ vs. the non-dimensional radial distance for different heights in the z -direction ($\bar{z} = 0$ solid line, $\bar{z} = 1/4$ dashed line, $\bar{z} = 1/2$ dash-dotted line). $\bar{\beta} = 0.25$ (a) $\bar{\beta} = 1.0$, (b) $\bar{\beta} = 4.0$ (c).

According to Arnol'd's theorem, a solution of Euler's equation will be stable if the integral representing the second-order variation $\delta^2 E$ in kinetic energy is positive definite or negative definite (Davidson 1994). We consider a kinetically admissible, infinitesimally small, solenoidal and axisymmetric displacement field $\delta\eta$ applied to the fluid elements, so that the circulation on a small area element remains unchanged by the displacement. Then, it can be shown that the second-order variation in kinetic energy is

$$\delta^2 E = \frac{1}{2} \int_V [\delta\mathbf{v} \cdot \delta\mathbf{v} + \delta\boldsymbol{\eta} \cdot (\delta\boldsymbol{\omega} \times \mathbf{v})] dV. \quad (3.10)$$

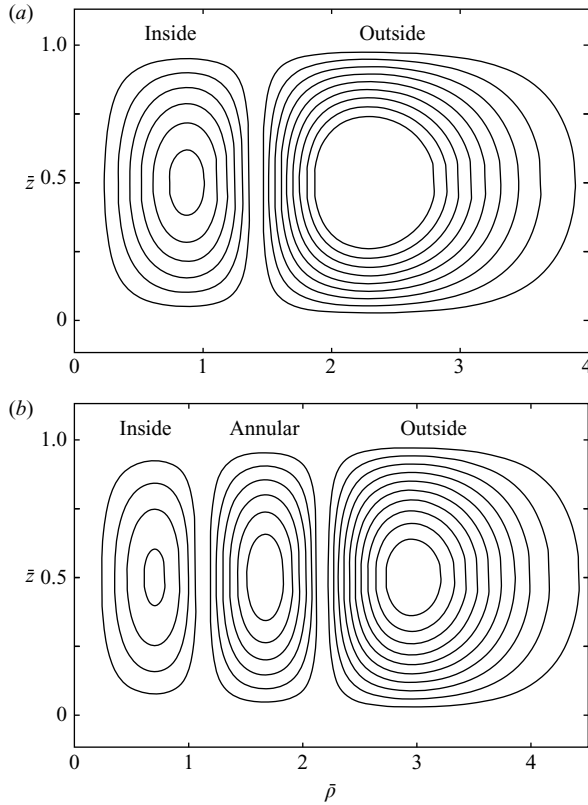


FIGURE 5. Projections of streamlines on the (ρ, z) -plane for vortices with axial and toroidal circulations confined between two horizontal parallel plates and impermeable vertical cylindrical surfaces. (a) corresponds to the radial mode $n=2$ where the flows inside and outside of one impermeable cylindrical surface are indicated. For (b) ($n=3$), an additional annular region exists which is confined between two vertical cylindrical surfaces.

Here, $\delta \mathbf{v}$ and $\delta \boldsymbol{\omega}$ are the first-order variations in velocity \mathbf{v} and vorticity $\boldsymbol{\omega}$

$$\delta \mathbf{v} = \delta \boldsymbol{\eta} \times \boldsymbol{\omega} + \nabla \delta s, \quad \delta \boldsymbol{\omega} = \nabla \times (\delta \boldsymbol{\eta} \times \boldsymbol{\omega}). \quad (3.11)$$

The scalar field $\nabla \delta s$ is such that $\delta \mathbf{v}$ is divergence free.

The positive or negative definiteness of $\delta^2 E$ for any arbitrary $\delta \boldsymbol{\eta}$ is the sufficient condition to ensure stability. If this condition cannot be satisfied, the flow field will be potentially, but not necessarily, unstable. To check Arnol'd's condition, we first replace all the related quantities in terms of ψ_2 . Then, applying the standard procedures (Mestel 1989; Davidson 1994) to our problem, we find a lower and upper bound for $\delta^2 E$:

$$\frac{1}{2} \int_V \delta \boldsymbol{\eta} \cdot \mathbf{T}^- \cdot \delta \boldsymbol{\eta} \, dV \leq \delta^2 E \leq \frac{1}{2} \int_V \delta \boldsymbol{\eta} \cdot \mathbf{T}^+ \cdot \delta \boldsymbol{\eta} \, dV \quad (3.12)$$

where \mathbf{T}^- and \mathbf{T}^+ are two second-order symmetric tensors

$$\mathbf{T}^- = \left(\frac{\lambda^2}{\rho^2} - \beta^4 \right) \nabla \psi_2 \nabla \psi_2 + \nabla \psi \nabla \frac{\hat{L}(\psi_2)}{\rho^2} + \nabla \frac{\hat{L}(\psi_2)}{\rho^2} \nabla \psi, \quad \mathbf{T}^+ = \left(\beta^4 - \frac{\lambda^2}{\rho^2} \right)^2 \rho^2 \psi^2 \mathbf{I} + \mathbf{T}^-. \quad (3.13)$$

Therefore, if it can be shown that either \mathbf{T}^- is positive definite or \mathbf{T}^+ is negative definite, the flow fields can be considered to be stable under external perturbations.

It is well known that the flow with axial and toroidal swirl does not satisfy Arnold's condition globally (Moffatt 1990; Davidson 1994). This indicates that in general these systems are potentially unstable. This is true for the radial order $n = 1$ and $n = 2$ where the stability cannot be assured. It seems that the three-dimensional velocity fields inside or outside an axially confined cylinder are potentially unstable. However, the flows with $n > 2$ have several intermediate segmented subdomains which are confined in annular regions and disconnected from each other by impermeable cylindrical walls. Velocity fields in such regions seem to be stable for large values of $\bar{\beta}$. The physical explanation of such behaviour is simple. Because of the centrifugal instability, circulating flows with axial swirl are generally unstable in the region where the angular momentum decreases with radius (Rayleigh 1916). Hence, if $\bar{\beta}$ is sufficiently high that ϵ (a measure of angular momentum) is sufficiently low (figure 1), the resulting centrifugal instability can be effectively suppressed by two confining vertical cylinders. We numerically check the eigenvalues of \mathbf{T}^+ and \mathbf{T}^- to quantify this effect. We find that the middle region for $n = 3$ is stable for $\bar{\beta} > 6.7$. Similarly, for $n = 4$, the second and the third subdomains with increasing radial distances are stable for $\bar{\beta} > 7.4$ and $\bar{\beta} > 8.1$, respectively. However, a general stability condition for these flows with arbitrary order is yet to be determined. Also, in real flow phenomena, the presence of small viscous dissipation can affect the stability. We believe that the viscous effect will tend to stabilize the system more and we will analyse this in the near future.

4. Superposed flow fields with axial and toroidal circulations

The proposed linear model provides a complete set of basis solutions for swirling flows. These basis functions can be used to expand complicated velocity fields with frequent spatial fluctuations. Such expansions can be useful in the study of turbulent vortices.

If we superpose the proper solutions corresponding to different radial modes (n) and axial wavenumbers (m) in a specific manner, we can construct complicated but steady vortical structures. The velocity fields in such vortices, though steady, mimic an instantaneous flow field in a real turbulent phenomenon with frequent spatial fluctuations. In this section, we describe the particular superposition procedure and present a couple of cases where this procedure is applied.

4.1. Superposition of flows with different radial modes

We consider a linear combination of the solutions given by (3.1)

$$\psi_2 = \sum_{m=1}^M A_m \sin(m\pi\bar{z})\tilde{h}_n(\eta)e^{-\eta/2}, \quad (4.1)$$

or of the solutions with a phase difference in the sinusoidal dependence along \bar{z} ,

$$\psi_2 = \sum_{m=0}^M A_m \cos(m\pi\bar{z})\tilde{h}_n(\eta)e^{-\eta/2}. \quad (4.2)$$

Here, $M > 1$ is an integer and A_m is the spectral amplitude which is in general dependent on m . The polynomial \tilde{h}_n is a renormalized function so that

$$\tilde{h}_n = \frac{h_n}{n!}. \quad (4.3)$$

The order of the radial mode n is a function of m , and denoted as n_m here in after.

According to (2.18), for given values of $\bar{\lambda}$ and $\bar{\beta}$, the integer numbers n_m and m in (3.1) should satisfy the following relation

$$\bar{\lambda}^2 = 4n_m\bar{\beta}^2 + m^2\pi^2. \quad (4.4)$$

We are interested in those values of $\bar{\lambda}$ and $\bar{\beta}$ for which it is possible to find an integer number for n_m corresponding to each possible integer value of m in the interval $[-M, M]$ so that (4.4) is satisfied. Then it can be proved that

$$\bar{\lambda} = \sqrt{\frac{p_\lambda}{q}} \pi, \quad \bar{\beta} = \sqrt{\frac{p_\beta}{lq}} \frac{\pi}{2}, \quad (4.5)$$

where p_λ , p_β , q and l are all integers. The calculations can be simplified if an additional constraint in the form of $p_\beta = 1$ is assumed. This helps us to find simple expressions for n_m and M in terms of m , p_λ , q and l

$$n_m = l(p_\lambda - m^2q) \quad M = \text{Int}(\sqrt{p_\lambda/q}), \quad (4.6)$$

where Int denotes the largest integer which is smaller than the argument. These expressions give all the necessary relations that are required to properly superpose solutions for a particular $\bar{\lambda}$ and $\bar{\beta}$.

4.2. Flow fields with different spectral distributions

We use (4.6) to describe two different fields. For both cases, we assign the values of the integer parameters as below

$$p_\lambda = 30, \quad q = 1, \quad l = 1. \quad (4.7)$$

Hence, we find $M = 5$ and $n_m = 30, 29, 26, 21, 14, 5$ for $m = 0, 1, 2, 3, 4, 5$ from (4.6).

The first of the two cases is referred as the Gaussian spectral distribution where the spectral amplitude A_m is described by a Gaussian distribution

$$A_m = \exp[-m^2\pi^2\bar{\sigma}^2], \quad (4.8)$$

where $\bar{\sigma}$ is a dimensionless parameter. Then this expression for the amplitude is used in (4.2) to evaluate the flow-related quantities. The second case corresponds to (4.1) with a Maxwellian distribution of the spectral amplitude

$$A_m = m\pi \exp[-m^2\pi^2\bar{\sigma}^2]. \quad (4.9)$$

The parameter $\bar{\sigma}$ is considered to be 0.25 for both cases.

The flow fields corresponding to (4.8) and (4.9) represent two different physical situations. For (4.9), the vortical system is similar to those described in §3, where the flow domain is axially bounded by two parallel walls. In such a case, vorticity is generated by a vorticity generator which in a real-life condition should compensate for any small loss due to boundary-layer dissipation at the confining surfaces. In contrast, the Gaussian spectrum in (4.8) is associated with an open system where the flow field is periodic in the axial direction. Physically, this is equivalent to a flow with widely separated entry and exit so that vorticity enters through the entrance plane, leaves the domain at the exit and creates repeating vortical structures in between. If

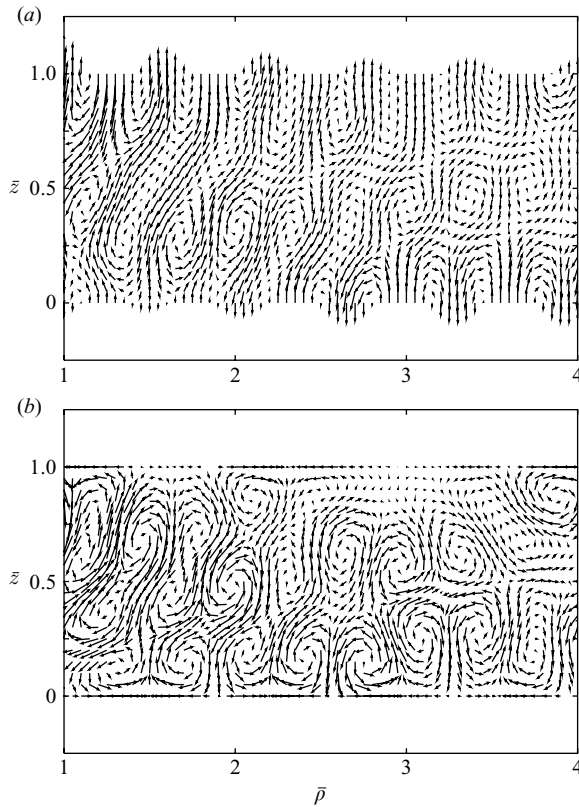


FIGURE 6. Projections of velocity fields in the (ρ, z) -plane for vortices with axial and toroidal circulations. (a) Gaussian and (b) Maxwellian spectra.

there is a small dissipation in the system, it is manifested by a small decay in the total head along the axial direction.

For the Gaussian spectral distribution, the tangential velocity in the ρ -direction vanishes at $\bar{z}=0$ and $\bar{z}=1.0$, whereas the flow in the second case satisfies the no-penetration condition at the same planes. The projections of streamlines in the (ρ, z) -plane illustrate these facts in figure 6. In both cases, the velocity field shows complex structures of small-scale circulations. For the Gaussian spectra, these vortical patterns are more elongated in the z -direction and are wavy because in this case flow can penetrate the boundary and thus has more freedom in the vertical direction. In contrast, for the Maxwellian spectra, the structures are more compact to ensure mass conservation between the impermeable boundaries. We choose a window from $\rho=1.0$ to $\rho=4.0$ in order to show the structural complexity in detail. However, in any region of the flow domain, we can see such complex circulations unless the window of observation is far away from the axis of symmetry where the fluid mechanical quantities decay to zero.

In figure 7, we present the dimensionless velocity component (\bar{v}_ϕ) in the angular direction and the dimensionless pressure \bar{p} as functions of $\bar{\rho}$ for different \bar{z} . Both fields are highly fluctuating for either of the spectral distributions. The pressure field has a more frequent fluctuation compared to v_ϕ because the difference in pressure scales as the difference in the square of the velocity. Hence, the pressure should fluctuate roughly twice as much as v_ϕ . For Maxwellian spectra, v_ϕ is zero at $\bar{z}=0$ and $\bar{z}=1.0$

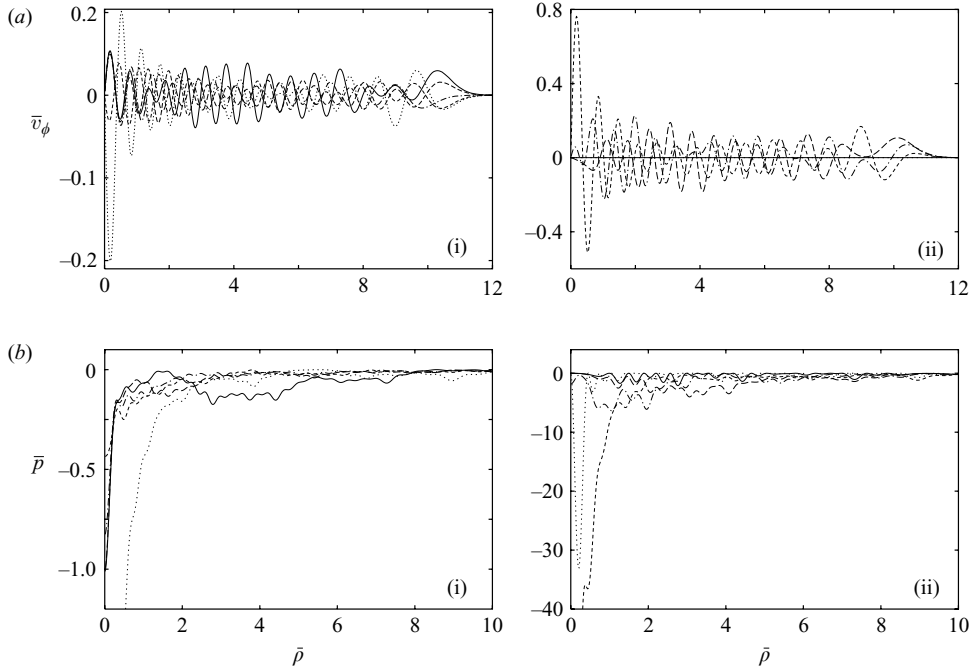


FIGURE 7. (a) Velocity in the ϕ direction and (b) pressure are presented as functions of $\bar{\rho}$ for different \bar{z} ($\bar{z}=0$ solid, $\bar{z}=0.25$ long-dashed, $\bar{z}=0.5$ dash-dotted, $\bar{z}=0.75$ short-dashed, $\bar{z}=1.0$ dotted). (i) Gaussian spectra and (ii) Maxwellian spectra.

along with v_z . Near the axis of symmetry, both flows have a large suction pressure to sustain the circulations.

5. Conclusion

We propose a linear model to analyse various types of three-dimensional flows with axial swirl and toroidal circulation. Our formulation enables us to represent the vortical systems by a linear homogeneous partial differential equation with only one dependent variable. This equation is similar to the equation involved in the hydrogen problem in quantum mechanics, and gives regular and localized solutions. Owing to the nature of the governing equation, a quantization relation, (2.18), can be derived between the strengths of specific energy and specific angular momentum in the axial direction.

We use our model to address several fluid mechanical problems. First, we focus on vortical circulations with axial and toroidal swirls trapped in the regions bounded by planar and cylindrical surfaces. We consider flow fields between two infinite parallel impermeable walls, as well as vortices bounded by an axially confined cylinder or annulus. Each of these geometries corresponds to a basis solution of the governing scalar equation. The results agree qualitatively with three-dimensional circulations in vortex simulators and exponentially decaying far fields produced by rotary machines such as fans or propellers.

In the aforementioned real systems, vorticity is generated in an inner region (near the injector or rotor, depending on the problem). The inviscid solution is not valid

there. However, if the Reynolds number is sufficiently high, the inviscid assumption is valid far away from the core. This far field has both axial and toroidal swirls where the vorticity is convected from the inner region. In reality, there are also boundary layers at the confining surfaces. The viscous loss in such boundary layers is compensated by the vorticity generator. This energy-balance consideration must be taken into account in order to apply our solutions effectively in the analysis of vortical systems.

If the derived solutions are superposed in a proper manner, they can form steady but complicated structures. We apply this superposition procedure to construct two different velocity fields. Streamlines of these constructed flows show a convoluted pattern. We also notice frequent spatial fluctuations in both pressure and velocity which resemble instantaneous fields involved in turbulent processes.

The presented solutions form a complete set of basis functions corresponding to axial and toroidal circulations. Hence, any complicated flow can be expanded in terms of these fields. Such expansions can be used to simulate large-scale systems with temporal fluctuations. However, the applicability of the method can be increased considerably, if the effect of near-wall viscous dissipation can be incorporated into the solutions.

The viscous dissipation at a solid surface can be studied by using the boundary-layer theory. In the boundary-layer formulation, the derived fields can be treated as the outer solutions far away from the wall. Then the far field can be used to find the matching boundary condition for the inner viscous solution near the solid surface. This will enable us to extend the present analysis to high-Reynolds-number swirling flows where the viscous effect is only important near a wall and can be neglected everywhere else.

REFERENCES

- ARNOLD, V. I. 1966a On an *a priori* estimate in the theory of hydrodynamical stability. *Izv. Vyssh. Ucheb. Zaved. Matematika* **79**, 267–269.
- ARNOLD, V. I. 1966b Sur un principe variationnel pour les écoulements stationnaires des liquides parfaits et ses applications aux problèmes de stabilité non linéaires. *J. Méc.* **5**, 29–43.
- BATCHELOR, G. K. 1964 Axial flow in trailing line vortices. *J. Fluid Mech.* **20**, 645–658.
- BAZZANT, M. Z. & MOFFAT, H. K. 2005 Exact solutions of the Navier–Stokes equations having steady vortex structure. *J. Fluid Mech.* **541**, 55–64.
- BRAGG, S. L. & HAWTHORNE, W. R. 1950 Some exact solutions of the flow through annular cascade actuator disks. *J. Aero. Sci.* **17**, 243–249.
- BUNTINE, J. D. & SAFFMAN, P. G. 1995 Inviscid swirling flow and vortex breakdown. *Proc. R. Soc. Lond.* **449**, 139–153.
- BURGGRAF, O. R. & FOSTER, M. R. 1977 Continuation or breakdown in tornado-like vortices. *J. Fluid Mech.* **80**, 685–704.
- CHURCH, C. R., SNOW, J. T., BAKER, G. L. & AGEE, E. M. 1979 Characteristics of tornado-like vortices as a function of swirl ratio: a laboratory investigation. *J. Atmos. Sci.* **36**, 1755–1776.
- DAVIDSON, P. A. 1994 Global stability of two-dimensional and axisymmetric Euler flows. *J. Fluid Mech.* **276**, 273–305.
- DELBENDE, I., CHOMAZ, J. M. & HUERRE, P. 1998 Absolute/convective instability in the Batchelor vortex: a numerical study of the linear impulse response. *J. Fluid Mech.* **355**, 229–254.
- EMANUEL, K. A. 1991 The theory of hurricanes. *Annu. Rev. Fluid Mech.* **23**, 177–196.
- ESCUDIER, M. 1984 Observations of the flow produced in a cylindrical container by a rotating endwall. *Exps. Fluids* **2**, 189–196.
- ESCUDIER, M. 1987 Confined vortices in flow machinery. *Annu. Rev. Fluid Mech.* **19**, 27–52.
- FERNANDEZ-FERIA, R., DE LA MORA, J. F. & BARRERO, A. 1995 Solution breakdown in a family of self-similar nearly inviscid axisymmetric vortices. *J. Fluid Mech.* **305**, 77–91.

- FRAENKEL, L. E. 1956 On the flow of rotating field past bodies in a pipe. *Proc. R. Soc. Lond.* **233**, 506–526.
- FUKADA, R., NIGIM, H. & KOYAMA, H. 1996 Measurements and visualization in the flowfield behind a model propeller. *J. Aircraft* **33**, 407–413.
- GELFGAT, A. Y., BAR YOSEPH, P. Z. & SOLAN, A. 1996 Stability of confined swirling flow with and without vortex breakdown. *J. Fluid Mech.* **311**, 1–36.
- GOLDSHTIK, M. A. & SHTERN, V. N. 1990 Collapse in conical viscous flows. *J. Fluid Mech.* **218**, 483–508.
- GOLLUB, J. P. & SWINNEY, H. L. 1975 Onset of turbulence in a rotating fluid. *Phys. Rev. Lett.* **35**, 927–930.
- GRIFFITHS, D. J. 1994 *Introduction to Quantum Mechanics*. Prentice-Hall.
- HILL, M. J. M. 1894 On a spherical vortex. *Phil. Trans. R. Soc. A* **185**, 213–245.
- KELLER, J. J. 1994 Entrainment effects in vortex flows. *Phys. Fluids* **6**, 3028–3934.
- LAMB, H. 1945 *Hydrodynamics*. Dover.
- LE DIZÈS, S. & LACAZE, L. 2005 An asymptotic description of vortex Kelvin modes. *J. Fluid Mech.* **542**, 69–96.
- LEPICOVSKY, J. & BELL, W. A. 1984 Aerodynamic measurements about a rotating propeller with a laser velocimeter. *J. Aircraft* **21**, 264–271.
- LONG, R. R. 1961 A vortex in an infinite viscous fluid. *J. Fluid Mech.* **11**, 611–623.
- LOPEZ, J. M. 1998 Characteristics of endwall and sidewall boundary layers in a rotating cylinder with a differentially rotating endwall. *J. Fluid Mech.* **359**, 49–79.
- MALIK, M. & CHANG, C. L. 1994 Crossflow disturbances in three-dimensional boundary layers: nonlinear development, wave interaction, and secondary instability. *J. Fluid Mech.* **268**, 1–36.
- MESTEL, A. J. 1989 On the stability of high-Reynolds-number flows with closed streamlines. *J. Fluid Mech.* **200**, 19–38.
- MITSUMA, Y. & MONJI, N. 1984 Development of a laboratory simulator for small-scale atmospheric vortices. *Nat. Disaster Sci.* **6**, 43–54.
- MOFFATT, H. K. 1981 Some developments in the theory of turbulence. *J. Fluid Mech.* **106**, 27–47.
- MOFFATT, H. K. 1990 Structure and stability of solutions of the Euler equations: a Lagrangian approach. *Phil. Trans. R. Soc. Lond. A* **333**, 321–342.
- RAYLEIGH, LORD 1916 On the dynamics of revolving fluids. *Proc. R. Soc. Lond. A* **93**, 148–154.
- SAFFMAN, P. G. 1992 *Vortex Dynamics*. Cambridge University Press.
- SHTERN, V. N. & HUSSAIN, F. 1999 Collapse, symmetry breaking and hysteresis in swirling flows. *Annu. Rev. Fluid Mech.* **31**, 537–566.
- SOZOU, C., WILKINSON, L. L. & SHTERN, V. N. 1994 On conical swirling flows in an infinite fluid. *J. Fluid Mech.* **276**, 261–271.
- SQUIRE, H. B. 1956 *Surveys in Mechanics: Rotating Fluid*. Cambridge University Press.
- WANG, C. Y. 1991 Exact solutions of the steady-state Navier–Stokes equation. *Annu. Rev. Fluid Mech.* **23**, 159–177.
- WARD, N. B. 1972 The explanation of certain features of tornado dynamics using a laboratory model. *J. Atmos. Sci.* **29**, 1194.